TOPICAL REVIEW

Recent Start-Up Techniques Intended for TEG Energy Harvesting: A Review

MAHMOUD AHMED[ID][1], **(Member, IEEE), SEBASTIEN GENEVEY**[ID][2],
MOHAMED ALI[ID][1], **(Member, IEEE), YVON SAVARIA**[ID][1], **(Life Fellow, IEEE),**
AND YVES AUDET[ID][1], **(Member, IEEE)**
[1]Department of Electrical Engineering, Polytechnique Montréal, Montreal, QC H3T 1J4, Canada
[2]Dolphin Design (formerly Dolphin Integration), 38240 Meylan, France

Corresponding author: Mahmoud Ahmed (mahmoud.ahmed@polymtl.ca)

ABSTRACT The growing number of energy-autonomous applications raises the need for reliable DC energy harvesting techniques such as Thermoelectric Generators (TEGs). One key issue, however, is the minimum voltage (40–60 mV) required for start-up in small TEG energy harvesting sources. We review in this paper recent start-up solutions for TEG energy harvesting technologies. Different solutions have been categorized into 5 main approaches: external battery, extra-fabrication-process-based, transformers, multisource energy harvesting, and DC-AC-DC conversion using oscillators. The ''DC-AC-DC conversion ring oscillators'' approach is then shown to be the most promising solution in line with DC energy harvesting applications because it offers several advantages over other approaches, such as allowing full integration with good performance, compatibility with regular CMOS technology, and lower cost. Then, its different implementations are discussed and a detailed analysis is provided to identify their respective advantages and limitations.

INDEX TERMS TEG, EH, start-up techniques, ring oscillator, Schmitt Trigger, IoT, DC-AC conversion.

I. INTRODUCTION

There is a pressing need for extending battery lifetime or -preferably- achieving battery-less operation for numerous potential applications such as wireless sensors, Internet of things (IoT), and Artificial Intelligence of Things (AIoT). Devices in these applications should allow non-stop operation for extended periods [1], [2], [3], [4], [5]. To extend battery lifetime, much effort was put into developing techniques to reduce power consumption, such as sleep and deep-sleep operations modes [6], Dynamic Voltage and Frequency Scaling (DVFS) [7], Adaptive Body Bias (ABB) [8], and event-based monitoring [9]. Nevertheless, the existence of batteries in the aforementioned systems is still associated with replacement costs and reliability issues, especially in applications where replacing the battery is physically challenging, like in implanted biomedical devices or remote

The associate editor coordinating the review of this manuscript and approving it for publication was Michail Kiziroglou[ID].

devices in sea or space [10], [11]. Thus, achieving battery-less operation is more favorable, and can be established by converting ambient energy into electric energy [12], [13].

The procedure of converting energy from ambient sources into electrical energy is called Energy Harvesting (EH) [14]. Some examples of available ambient sources of energy are electromagnetic radiation (such as light [15], [16], and Radio Frequency (RF) waves [17], [18], thermal gradients [19], and mechanical motion [20]). Harvesting mechanical motion requires vibrating media, which is not available in many applications. On the other hand, the most abundant sources of energy are RF waves and thermal energy [21], [22], [23]. RF energy is abundant in populated areas since billions of wireless devices radiate RF waves constantly. RF energy is emitted by satellites, mobile phones, WiFi routers, etc. However, ambient RF energy density in free space is limited [24], [25], [26]. Furthermore, Power Conversion Efficiency (PCE) in RF energy harvesters is also limited, because antennas of RF harvesters receive very

low RF power density due to propagation losses [27], [28]. Moreover, attenuation becomes worse with multi-path fading effects and longer distances [14], [29]. On the other hand, sources of energy, such as light and heat, are available in numerous environments, but they usually provide low voltage levels [30], [31].

Harvesting ambient thermal energy using TEGs is a convenient means of supplying power to many applications because it is scalable, reliable, and does not employ moving parts in contrast to vibration energy transducers [32], [33], [34]. Therefore, it is appealing in human body-powered biomedical devices such as pacemakers, which can be powered from thermal gradient across the human skin [35], [36], [37]. Also, on-chip TEGs can be used to harvest electrical energy from components waste heat, or any other heat source such as solar radiation or industrial waste heat [38], [39], [40]. However, TEG usually requires a constant temperature gradient, which is difficult to maintain unless there is a heat sink applied to one of the TEG's two sides. Also, for small temperature differences, the limited TEG output voltage (40-60 mV) forces the system to self-start-up from low voltage levels ($\approx 50\ mV$) [41], [42], [43].

As illustrated in Fig. 1, this paper categorizes different reported start-up approaches for DC energy harvesting technologies (TEGs as primary example) into 5 main types: external battery, extra fabrication process-based, transformers-based, multisource energy harvesting, DC-AC-DC conversion using oscillators. Then, it reviews the different implementations of the most promising approaches in line with energy harvesting applications. A detailed analysis of reported solutions is provided and discussed.

In the remaining parts of the paper, we introduce our classification of TEGs start-up techniques in Section II. A detailed analysis of the DC-AC-DC conversion using the oscillator approach is presented in Section III, where the measured performances of the reported integrated solutions are summarized and compared. Our results and evaluation of the reviewed techniques are presented in Section IV. Finally, the paper is concluded in Section V.

II. TEG HARVESTER START-UP TECHNIQUES
First, we present briefly the operation principle of TEGs and the role of their start-up circuit in TEG harvesting systems. Then, we classify the start-up techniques into five main categories.

A. TEG OPERATION PRINCIPLE
As shown in Fig. 2(a), TEGs (also called Seebeck generators) are devices that convert heat (temperature differences) directly into electricity based on the Seebeck effect [19], [44]. According to that effect, the generated voltage is proportional to the temperature gradient between its two sides [45]. Unlike the Pyroelectric (PR) effect (which is based on the re-orientation of dipoles triggered by temperature fluctuations [44]), the ThermoElectric (TE) effect generates

a DC output [1]. Fig.2(b) illustrates a thermocouple, which is the basic construction unit of the thermal harvester. The principle of operation of a thermocouple is simple and is based on the Seebeck effect that generates electron-hole pairs [46] as follows: upon applying temperature difference across the junction of two dissimilar materials, heat flows from the hot to the cool side. Consequently, the energy that comes from the heat forces the free electrons and holes to move, forming an electrical potential across the junction that causes electrical current to flow in the case of a closed circuit [47]. Thus, the electrical potential (in volts) of the junction can be expressed as:

$$U = \alpha N(Ta - Te). \tag{1}$$

where Ta - Te is the temperature difference across the junction, α (in volt per Kelvin) is the Seebeck coefficient corresponding to a specific pair of materials, and N is the number of thermocouples in a TEG [48]. A voltage source in series with an internal resistance is representative of TEG model [49], [50] as shown in Fig. 2(c). The open-circuit output voltage of the TEG is proportional to the temperature gradient as indicated by equation 1 [51].

The use of TEGs for sensors, body-wearable applications, or implantable applications typically limit the output voltage to 40-60 mV (rarely exceeding 100 mV) for temperature differences of 1-2 K found between the body and ambiance. Thus, the system has to accomplish self-start-up from low voltage level $\approx 50mV$ [30], [53], [54]. This very low output voltage cannot power conventional CMOS electronic circuits, which calls for a high-efficiency voltage multiplier circuit (boost DC-DC converter) to successfully boost the output voltage to the desired value [30]. Fig. 3 depicts a conventional DC-DC boost converter. However, to start the main boost converter, it is required to have a DC voltage reservoir with a potential equal to or larger than 500 mV to power the remaining electronics. This can be achieved through a start-up circuit powered by the primary DC energy source [30], [55]. Additionally, lowering the startup voltage levels is significantly advantageous for boost converters because minimum input voltage for steady-state operation in most of the reviewed architectures is much less than 50 mV. Therefore, they can operate at much lower voltage levels (or thermal gradients) if they could properly start-up.

B. TEG HARVESTER START-UP TECHNIQUES CLASSIFICATION
Thus, we can categorize different reported start-up solutions for DC energy harvesting technologies (TEG as a primary example) into 5 main approaches as illustrated by Fig. 1:

1) EXTERNAL BATTERY
The first explored start-up technique consists of using an external specialized source of energy such as a battery [56], or pre-charged capacitor [57] to help start up the system for the very first time. Though this seems to be a simple
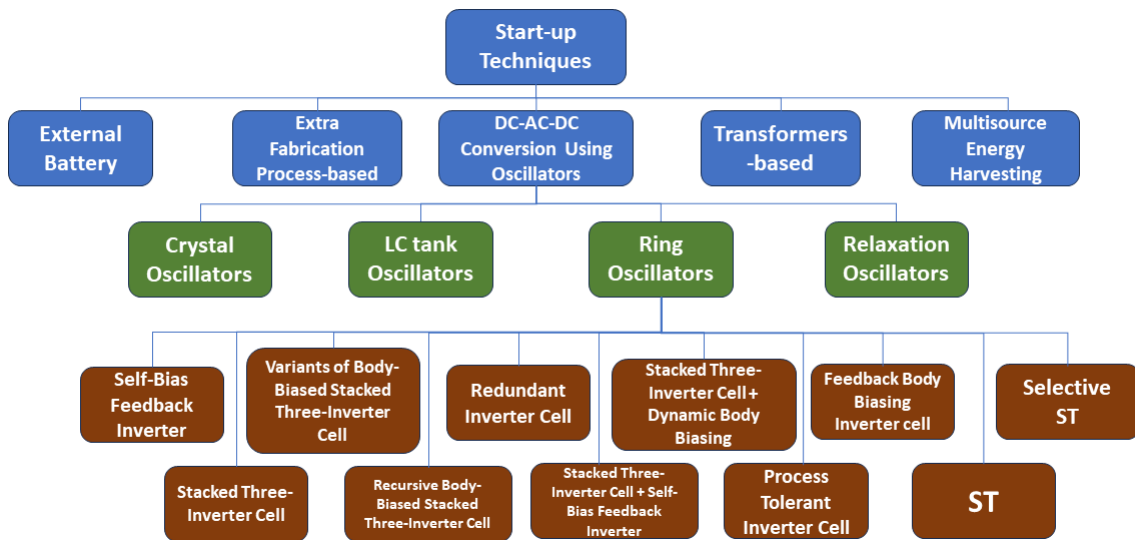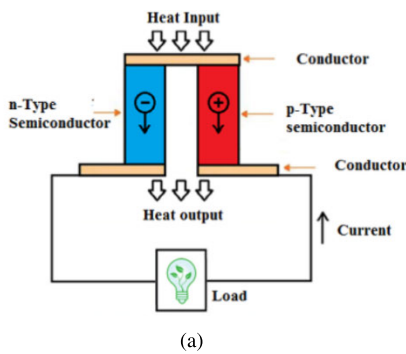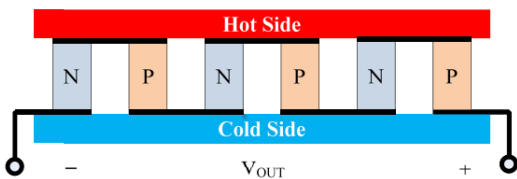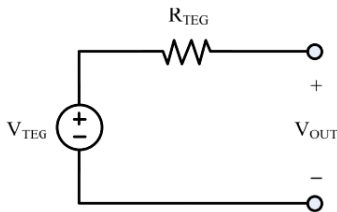
FIGURE 1. Classification of TEG harvester start-up techniques.

(a)

(b)

(c)

FIGURE 2. (a) Typical TEG architecture, (b) Thermocouple unit, and (c) TEG Electrical equivalent circuit [52].

FIGURE 3. Block diagram of conventional self-start for TEG boost converter with 5 start-up approaches illustrated.

nonfunctional. This is a serious issue, especially when the device is used in a remote place or implanted in a human body. Thus, the reliability and cost of such an approach constitute real obstacles. Some researchers attempted to address this problem by proposing battery-assisted energy harvesting systems to reduce the rate of battery replacement and to realize self-charging for the rechargeable battery [58]. Consequently, battery-assisted energy harvesting systems can significantly prolong the battery life compared with conventional battery-powered IoT nodes. However, the issue of battery replacement remains unsolved.

2) EXTRA FABRICATION PROCESS-BASED

The second approach attempts to solve the restart ability problem of the first approach by conducting extra fabrication processes or post-fabrication steps. For instance, implementing fabricated mechanical switches enabled starting up from a voltage level as low as 35 mV [47]. Also, some succeeded at compensating for the die-to-die process

solution, restarting the system would require some of the boost converter output to be saved for later, which limits the performance of the converter in addition to the risk of getting fully depleted of energy. This would render the whole system
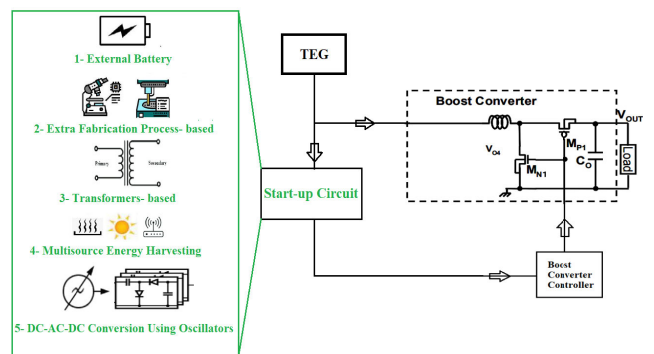
variation by applying post-fabrication threshold voltage trimming [54]. Although the use of mechanical switches enabled starting up from low voltages, and post-fabrication trimming reduced the minimum operating voltage of the start-up oscillator to 95 mV, the extra fabrication process steps add complexity and cost to the system, and it is incompatible with standard CMOS technologies provided by existing foundries. Moreover, implemented mechanical switches need a vibrating medium to operate, which limits their range of application significantly.

3) TRANSFORMERS-BASED

The third approach explores the use of transformers which comprise two inductors configured in mutual feedback. For instance, authors in [53] managed to start-up from a 40 mV source, then reused the transformer in the main converter by exploiting one of its two sides as an inductor. However, the efficiency of such a solution is very low and it does not compensate for the large area of the transformer. Also, work reported in [59] demonstrates the effect of designing the core of the DC-DC converter as a pulse transformer boost converter using a Dynamic Threshold MOS transistor (DTMOS). This system can self-start at 36 mV input voltage since employing DTMOS increases transistor saturation current and output power compared to conventional transistors at similar input voltage and improves power efficiency up to two times at sub-300 mV input voltages compared with a conventional configuration. Furthermore, transformer-based solutions have been widely adopted in industrial applications where the area is less significant than the minimum input voltage that allows system start-up. For example, the work presented in [60] is a transformer-based boost converter that operates from input voltages as low as 21 mV. Another highly integrated DC-DC converter was presented in [61] which operates from 20 mV with the ability to change such value by changing the primary-secondary turns ratio of the transformer. In [62] a transformer-based startup scheme with voltage monitors for energy harvesting at input voltage as low as 20 mV was reported. Although transformer-based techniques enable low start-up voltages, the use of bulky off-chip components renders them unsuitable for system integration or deep miniaturization. There were some attempts to use on-chip transformers. Work in [63] introduces a stacked-type transformer-based LC oscillator, but the limitation of low on-chip quality factor limits the input voltage to 160 mV and 25.8% efficiency, and to 100 mV and 33% efficiency in best cases as reported by [64]. Moreover, the authors in [65] propose an 85 mV input, fully integrated voltage multiplier, fabricated in 65nm CMOS, comprising a passive clock boost using on-chip transformers and an integrated LC oscillator. Despite achieving low input voltage, it is still out of range since the use of TEGs for most applications limits the minimum output voltage level to 40-60 mV for temperature differences of 1-2 K [19], [30], [53].

4) MULTISOURCE ENERGY HARVESTING

The fourth approach comprises the use of an additional energy harvester to realize the start-up of the system. For instance, authors in [66] use an off-chip antenna with auxiliary RF energy harvesting to start the system for the TEG boost converter to operate properly. A thermal/RF hybrid energy harvester was presented in [67]. It can harvest energy from a TEG and an RF energy source simultaneously, by using a rectifying combination technique and a modified Fractional Open-Circuit Voltage (FOCV) Maximum Power Point Tracking (MPPT) technique. Although the system works efficiently from a TEG input voltage as low as 50 mV, the RF power must be available simultaneously and continuously with the TEG power. Similarly, work presented in [68] proposed simultaneous scavenging of both RF and thermal energy in a mixed manner, where the harvested DC voltage from a thermal source is used to bias a diode to improve the diode's RF-DC power conversion efficiency. Nevertheless, this technique introduces the complexity of an antenna and an auxiliary RF energy harvesting design, in addition to the bulky off-chip components used.

5) DC-AC-DC CONVERSION USING OSCILLATORS

Finally, the fifth approach exploits DC-AC conversion by inserting an intermediate oscillator stage, then AC-DC conversion with a boosted level by a charge pump [69]. Two types of oscillators could be considered: resonant oscillators and waveform oscillators [70]. Resonant oscillators include crystal oscillators and LC tank oscillator topologies. However, crystal oscillators can neither be integrated nor tuned. On the other hand, LC oscillators can be used to implement start-up circuits. Authors in [69] reported a converter with $V_{IN,min} = 50$ mV for start-up using an LC-tank oscillator followed by a voltage multiplier. Also, work in [62] presented a self-startup power management Integrated Circuit (IC)-based on a boost converter integrated with its complete control circuitry, including MPPT capacity. This converter supports cold self-start from TEG at a minimum of 60 mV, using three startup phases, two power-on-reset (POR) signals for smooth transitions between the phases, and a Hartley oscillator that conventionally requires two separate inductors. These authors reused one from the boost converter to minimize off-chip components. Moreover, work in [66] reported a converter with $V_{IN,min} = 11$ mV for start-up using an Enhanced-Swing Ring Oscillator (ESRO), off-chip inductors, zero-V_{TH} transistors and a three-stage Dickson Charge Pump (DCP). Nevertheless, the aforementioned oscillator-based methods still require off-chip inductors. On the other hand, there are attempts to realize an LC tank using integrated inductors such as in [71]. However, integrated inductors consume a large silicon area. In addition, integrated inductors have low Quality factors (Q), which degrades their performance. A detailed description of recent ultra-low-voltage oscillators based on LC-tank topologies is presented in [72].

The other oscillator type introduced in [70] is Waveform oscillators, which include relaxation oscillator and Ring

Oscillator (RO) topologies. However, relaxation oscillators have poor phase noise performance compared to ROs. Moreover, ROs could be realized by transistors only, which results in a small silicon area and low power implementation [71]. Therefore, RO topologies are excellent candidates for realizing reliable and fully integrated start-up solutions. A main challenge, however, is to extend their use to extremely low supply voltages [30].

Oscillator-based start-up is the most efficient technique for starting-up from a single voltage source. It also requires less silicon area as it can be fully integrated without trading off performance. Moreover, it is compatible with CMOS technology and it can be implemented at a lower cost, which is a critical aspect since IoT and wireless applications put stringent constraints on the system cost. Table 1 summarizes the advantages and disadvantages of the reviewed techniques.

III. DC-AC-DC CONVERSION USING OSCILLATORS APPROACH

The main challenge faced when employing the RO start-up solution is that a simple inverter normally used as a delay element in conventional RO requires a relatively large supply voltage (a few hundred millivolts) to ensure its correct logic operation. This requirement is not practical for energy-constrained harvesting applications because the input voltage available from the energy source will be mostly unable to reach a supply voltage sufficient to properly activate cells. Thus, supply voltage reduction is advantageous for supply voltage-constrained applications. However, it is limited by on-to-off current ratios degradation observed with decreasing supply [30], [58], [74]. Many scientists have attempted to provide valid solutions for this issue by either adopting a new delay cell architecture or by applying new biasing mechanisms to existing structures. Certainly, others optimized the results by combining different delay cell architectures with different biasing techniques. We will analyze the most significant results from the past ten years in the upcoming section.

A. SELF-BIAS FEEDBACK INVERTER

An RO consisting of gain-enhanced Self-Bias Inverters (SBIs) was reported in [75]. The SBI is composed of two inverters: the main inverter and the feedback inverter as shown in Fig. 4(a). The feedback inverter controls the main inverter body bias voltage to improve the voltage gain. The principle of operation of this configuration is as follows: When V_{IN} is low, V_{OUT} becomes high, and the output voltage of the feedback inverter becomes low. Thus, $V_{TH,P}$ becomes low and $V_{TH,N}$ becomes high. Therefore, ΔV_{TH} becomes higher than 0 V. On the other hand, when V_{IN} is high, V_{OUT} becomes low, and the output voltage of the feedback inverter becomes high. Thus, $V_{TH,P}$ becomes high and $V_{TH,N}$ becomes low. Therefore, ΔV_{TH} becomes lower than 0 V. Thus, the Voltage Transfer Curve (VTC) of the SBI comes close to the two curves of $\Delta V_{TH} < 0$ and $\Delta V_{TH} > 0$, as shown in Fig. 4(b), and the voltage gain is improved. Measurement
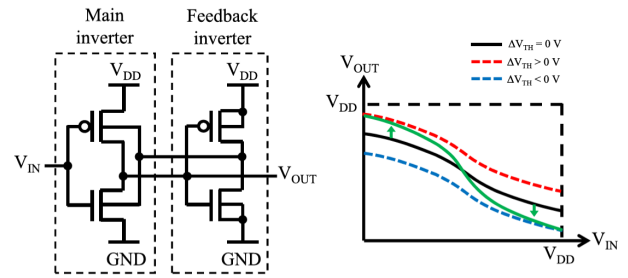

FIGURE 4. (a) Schematic of self-biased feedback inverter, and (b) its modified voltage transfer curve [75].
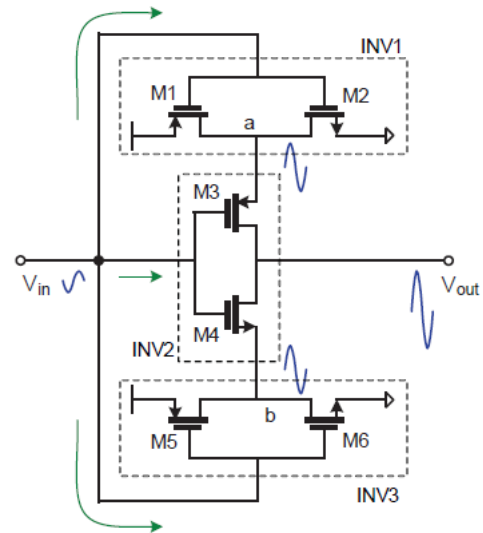

FIGURE 5. Stacked Three-Inverter Cell from [76].

results of this RO show its ability to oscillate at a low 42 mV supply voltage. This technique's main strength is that it can be applied to any delay cell (not limited to basic CMOS inverter) but at the expense of doubling the area and power consumption.

B. STACKED THREE-INVERTER CELL

A modified RO architecture using a stacked three-inverter delay element was presented in [76]. It can generate self-sustained oscillation from a 40 mV input supply voltage. As shown in Fig. 5, the delay element comprises three stacked inverters INV1, INV2, and INV3. The input signal is fed to all three inverters gates, and INV1 and INV3 outputs are connected to M3 and M4 sources, respectively. Additionally, the gate widths of M1 and M6 are larger than those of M3 and M4, respectively, to make the entire delay element DC operating point similar to that of a single inverter. Finally, INV2 consists of M3 and M4 only. The advantage of this topology is that it helps suppress the output leakage through the off switch by pulling the respective nodes to either V_{DD} or ground when the output needs to transition high or low, respectively. The implemented start-up oscillator, in 0.18 μm CMOS process, comprises 21 stages and it generates a clock

TABLE 1. Advantages and limitations of start-up approaches for TEG energy harvesting technologies.

Approach	Examples	Pros	Cons	References
External Battery	External Battery, pre-charged capacitor, battery-assisted EH systems	Simple, battery-assisted system reduces battery replacement rate and prolongs battery life by rechargeability	Limited performance, restarting is difficult (unreliable), expensive, battery replacement issues in remote/body implanted applications	[56]–[58]
Extra Fabrication Process based	Mechanical switches, post-fabrication threshold voltage trimming	Low start-up voltage (down to 35 mV), restarting the system autonomously, suppressing process variations effects	Extra fabrication process adds complexity and cost to the system, incompatible with standard CMOS technologies, limited application range (mechanical switches need a vibrating medium)	[47], [54]
Transformers-based	Off-chip transformer(s), pulse transformer boost converter using DTMOS, industrial products, integrated stacked-type transformer-based LC oscillator, voltage multiplier using on-chip transformers.	Low start-up voltage (down to 20 mV), restarting the system autonomously, possibility to reuse transformers as main boost inductor	Low efficiency, bulky (large area), unsuitable for system miniaturization, and limitation of on-chip quality factor limits the input voltage to 85 mV and 33% efficiency at best	[53], [59]–[65]
Multisource Energy Harvesting	Auxiliary RF energy harvester, thermal/RF hybrid energy harvester	Low start-up voltage (down to 50 mV), harvesting energy from (TEG) and (RF) energy source simultaneously, multisource energy harvesting is more reliable than one source	RF power that must be available simultaneously and continuously with the TEG power, added complexity of antenna and auxiliary RF energy harvesting design, bulky off-chip components.	[66]–[68]
DC-AC-DC Conversion Using Oscillators	LC oscillators (off-chip inductors), Hartley oscillator (off-chip inductors), ESRO using off-chip inductors, LC tank using integrated inductors, relaxation oscillator, crystal oscillators, ROs (will be reviewed intensively in table 2)	Low start-up voltage (down to 11 mV) using LC oscillators (off-chip inductors), RO has small area, consumes less power, fully integrated, start-up realization from one source only, compatible with regular CMOS technologies and less expensive, longer durability and better reliability	LC oscillators require off-chip inductors (Bulky + larger area), integrated inductors require a large silicon area with performance degradation due to low Q, relaxation oscillator has poor phase noise, crystal oscillators can neither be integrated nor tuned, ROs need to extend their use to extremely low supply voltages	[66], [69]–[71], [73]

frequency of 9.5 kHz with an 86% voltage swing from a 50 mV input supply voltage. Moreover, this proposed architecture's significance is that it allowed a variety of promising combinations of delay cells as we will see in the next few sections.

C. VARIANTS OF THE BODY-BIASED STACKED INVERTER

In [77], four new variants of a body-biased stacked inverter delay cell of [76] were proposed and implemented in 180nm BCD CMOS process. The delay cell comprises three inverters as shown in Fig. 6 (same as [76]). However, the body terminals of the ith stage are biased using one or a combination of V_{DD}, V_{SS}, Y_{i+1}, X_{i+1}, IN_{i+2} terminals. Fig. 6 depicts two adjacent delay cells in the RO (i^{th} and $i + 1^{th}$ stages). It also defines the terminology and the body terminals from which the operation of the device can be explained. 'B' refers to the body terminal of a MOSFET; 'p' ('n') following 'B' refers to the type of MOSFET under consideration. 'ST', 'SB', and 'M' respectively refer to "Stacked Bottom", "Stacked Top", or Middle inverter FETs. All stacked inverter variants have the same structure but with different Body connections. Their post-layout simulations show that the four

variants consume an average power of 24 pW at 50 mV. The NN-NN-NN variant, depicted in Fig. 6, has the highest swing that corresponds to 92% of its supply voltage, and the maximum gain per unit cell while it can start and sustain oscillations for a supply voltage as low as 32.5 mV. Among these variants, the fastest one can oscillate at a frequency of only 131.5 Hz.

D. RECURSIVE BODY-BIASED STACKED INVERTER

In [78], a recursive body-biased stacked inverter is introduced. These authors [76] propose to stack additional inverters at the top and bottom of the inverter recursively as shown in Fig. 7. The recursive-stacking technique increases the transconductance of the MOSFETs in the recursively stacked inverters as well as in the main inverter while decreasing leakage currents. This structure achieves low-voltage operation at the cost of an increased number of transistors, area, and power penalty. Their prototype test chip was fabricated in a 180-nm, 1-poly, 6-metal CMOS process technology with a deep n-well option. The measured lowest $V_{DD,min}$ was 26 mV, and all their prototype chips oscillated successfully at 30 mV.
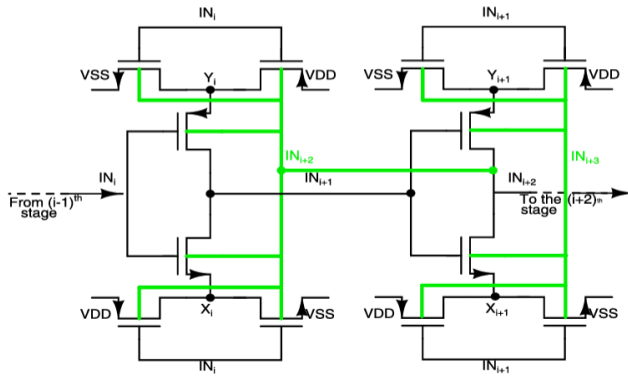
FIGURE 6. Two adjacent delay cells (i^{th} and $i + 1^{th}$ stages) in the NN-NN-NN Variant of the Body-Biased Stacked Inverter RO from [77].
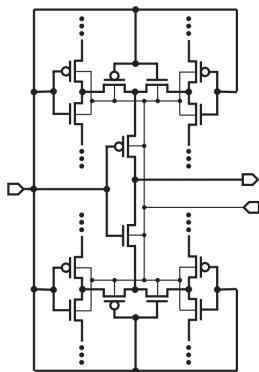

FIGURE 8. Two-stage redundant inverter from [79].

FIGURE 7. Recursive Body-Biased Stacked Inverter Cell from [78].
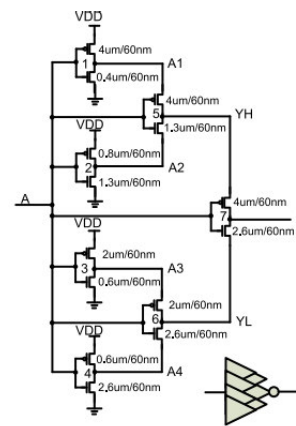
FIGURE 9. Three-stage redundant inverter from [79].

E. REDUNDANT INVERTER CELL

In [79], a redundant inverter RO is reported to self-oscillate at 45 mV. It is considered as an extension of the work presented in [76] as shown in Fig. 8. The 3-stage redundant inverter is shown in Fig. 9 and it is composed of 7 inverters. It is similar to the 2-stage redundant inverter but it generates a larger output swing and has the same working principle. Additionally, the authors claim that the concept can be easily extended to an N-stage redundant inverter. However, this comes obviously with more power and area consumption. The chip micrographs of this start-up system implemented in a 65nm CMOS technology are illustrated in Fig.10. The power converter proposed in [79] achieves 210 mV self-start voltage by implementing the 3-stage redundant inverter RO in the start-up circuit in three steps: The first RO and first charge pump have been used to achieve a low self-start of 60 mV, and the first charge pump produces an output around 105 mV during step 1. Then, a second RO and differential clock booster are optimized to drive the second charge pump, producing an output larger than 300 mV in step 2. Then, a clock divider and another clock booster are used in step 3 to generate an output clock offering 700 mV swing that is sufficiently large to drive the main converter. Although this power converter can sustain operation from 7 mV input, its start-up requirement of 210 mV is much
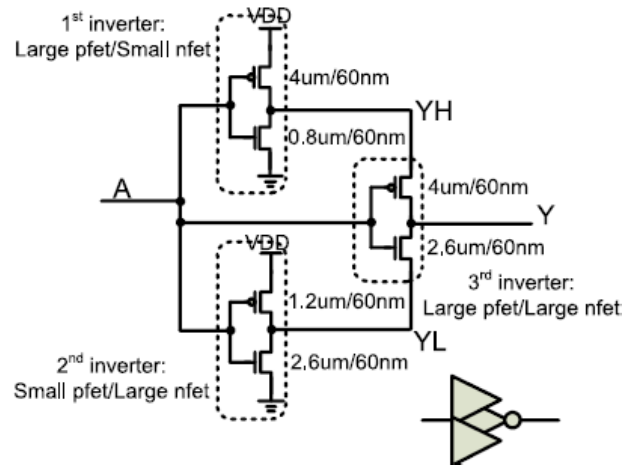
higher than the start-up voltage of the 2-stage redundant inverter (57 mV) reported in [76]. One possible reason is layout and measurement issues; another possible reason is that their overall start-up circuit implementation is not as optimum as the one reported in [76].

F. STACKED THREE-INVERTER CELL + SELF-BIAS FEEDBACK INVERTER

In [80], an RO composed of gain-enhanced Stacked Body Bias Inverters (SBBIs) is introduced. As shown in Fig. 11, the RO is composed of Stacked Body Bias Inverters (SBBIs) that are based on the conventional Self-Bias Inverter (SBI) from [75], and stacked three-inverter (SI) from [76]. This design was implemented in 0.18 μm CMOS process with a deep N-well option. Simulation results showed that the RO oscillates at 34 mV and generates a clock pulse with 88% voltage swing from a 50 mV supply voltage. The reported SBBI combines the advantages of both SBI and SI to enable oscillation at extremely low supply voltage since the voltage gain is improved by controlling the main inverter's supply (V_{DD} and GND) and body-bias voltages simultaneously.
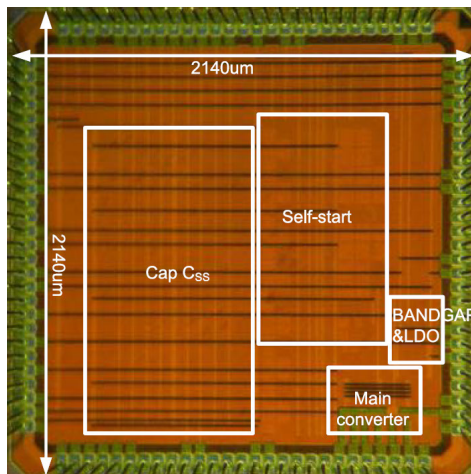
FIGURE 10. Chip micrograph of the fabricated redundant inverter cell implemented in 65nm CMOS process from [79].
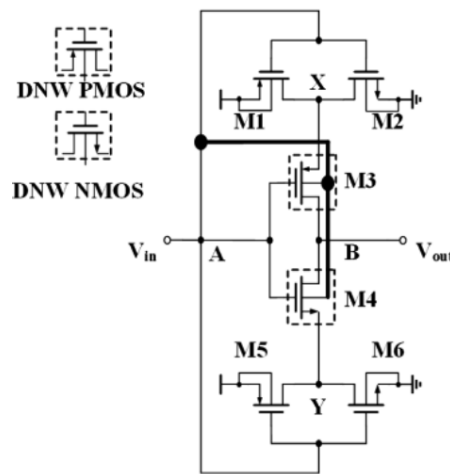

FIGURE 12. Stacked Three-Inverter Cell + Dynamic Body Biasing delay element from [58].
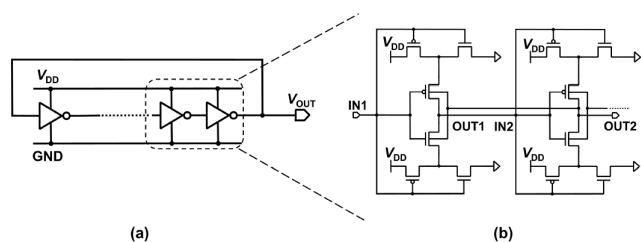

FIGURE 11. (a) RO from [80], and (b) individual delay cell composed from combining [75], [76] techniques.

G. STACKED THREE-INVERTER CELL + DYNAMIC BODY BIASING

An improved delay element based on work from [76] for cold start-up RO was reported in [58]. As shown in Fig. 12, all the transistors in the stacked inverter previously presented in [76] are replaced by Deep N Well (DNW) transistors. The body of all transistors is tied to the input node such that the threshold of those transistors is controlled by the input signal. Thus, by dynamically controlling the transistors' threshold voltage, the RO oscillates at a lower supply voltage. Furthermore, post-layout simulation results of this 21-stage RO show that it maintains oscillation under $V_{DD} = 36$ mV power supply, in addition to a wider swing compared with other cold start-up ROs. The authors extended their work to cover battery-assisted DC energy harvesting systems in [58] to reduce battery replacement frequency by realizing self-charging for rechargeable batteries. Thus, the battery-assisted energy harvesting system can significantly prolong battery life compared with conventional systems. This was achieved by inserting a low Voltage Level Shifter (VLS) to obtain a wider voltage range for biasing the body of the delay element presented in [3], to enhance both its Voltage Transfer Curve (VTC) and DC gain. Consequently, the cold start-up 21-stage RO of the modified delay element, implemented in 180 nm CMOS process, achieved oscillation under 24 mV V_{DD} under a typical corner at room temperature.

Although this design works with very low input voltage (the lowest reported for fully integrated start-up solutions), the issue of battery replacement remains.

H. PROCESS TOLERANT INVERTER CELL

The authors in [81] reported a successful start-up from a 60 mV voltage produced by a TEG by employing an RO and a 40-stage charge pump. They proposed a new process tolerant inverter cell, as depicted in Fig. 13, to be implemented in the RO and driver circuits to ensure functionality in different process corners. Fig. 14 shows the different corner cases' effects on the inverter cell. The inverter cell consists of a pull-up PMOS network and an NMOS pull-down network, consequently, the FS (fast-slow) and SF (slow-fast) corners oppositely affect these networks. Thus, these corners can result in inverter cell failure at small supply voltages. Therefore, they propose the inverter cell depicted by Fig. 13. To activate the auxiliary pull-up/down networks, a corner detection circuit is needed to generate the higher voltages necessary for their activation.

I. FEEDBACK BODY BIASING

In [19], some variations in the basic CMOS inverter cell were presented to reduce its threshold voltage. This is different from the "Self-bias feedback inverter" type reported in [75]. as there is no extra feedback stages to provide body biasing, instead, the body terminals of each NMOS and PMOS transistors of each stage are connected to the output voltage of the following stage as shown in Fig. 15,. For example, in the two consecutive stages N, and N+1; when the output voltage of stage N+1 transitions from low to high, the output voltage of stage N transitions from high to low. Consequently, the NMOS transistor of stage N turns on. As $V_{B,NMOS}$ is connected to the output voltage of stage N+1, the body voltage is high and the threshold voltage of the NMOS decreases, which aids the NMOS to turn ON faster. The same happens when stage N transitions from low to
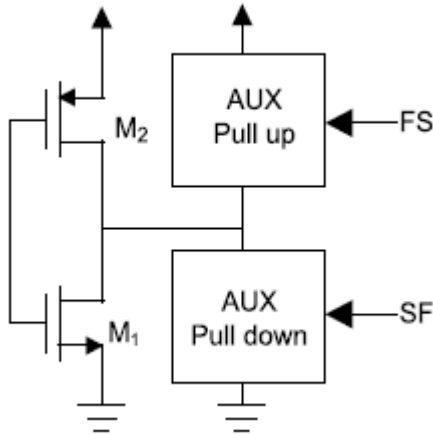
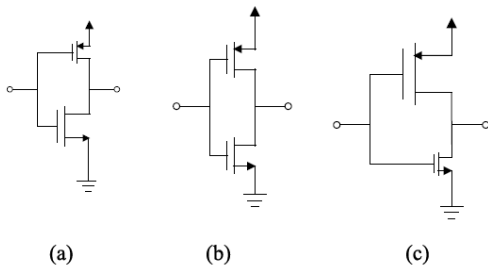**FIGURE 13.** Process-tolerant inverter cell from [81].

FIGURE 14. Inverter from [81] in different process corners (a) FS corner, (b) TT corner, and (c) SF corner.
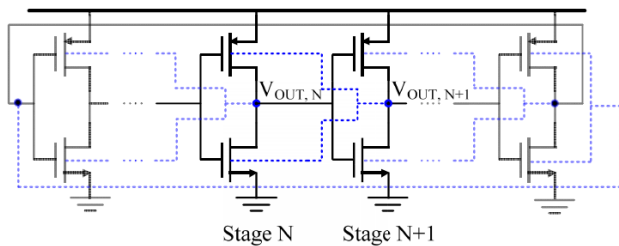

FIGURE 15. Schematic of RO from [19] employing feedback body biasing technique.

high. Therefore, a dynamic reduction in transistor threshold voltages leads to a decrease in V_{DD}. Consequently, these authors reached a minimum voltage of 60 mV for the correct operation of the bootstrap circuits and a maximum time of 400 ms for the circuit to start up.

J. SCHMITT TRIGGER DELAY CELL

The previously mentioned references either modify the basic inverter delay cell structure or its biasing to realize the RO used in TEG harvester start-up circuits. However, there is also a very promising class of delay cells derived from the Schmitt Trigger (ST) structure. First, we present a brief analysis of basic ST structure and operation, followed by a review
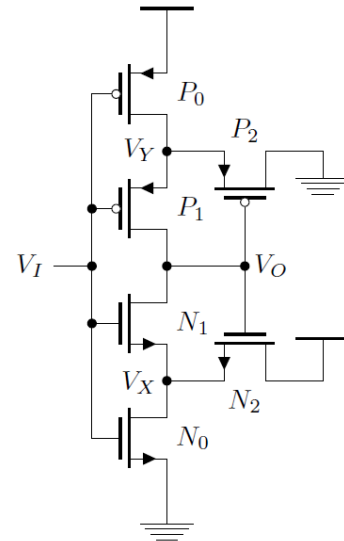

FIGURE 16. Basic ST delay element structure [82].

of recent applications in the subthreshold operating region, mainly on its application in TEG harvester start-up ROs.

1) ST STRUCTURE AND OPERATION

The classical CMOS ST is depicted in Fig. 16 [82]. Its operation in weak inversion is studied in detail in [83]. However, we can explain its operating principle roughly as follows: when the input is high, both N_0 and N_1 turn on, and the output is low because of the path between the output and the ground. This turns off N_2 and turns on P_2. Thus, V_Y becomes low and this helps suppress the leakage through P_0 and P_1 by establishing a positive feedback loop. Similarly, when the input is low, both P_0 and P_1 turn on, and the output is high because of the path between the output and V_{DD}. This turns P_2 off and turns N_2 on. Thus, V_X becomes high and this helps suppress the leakage through N_1 and N_0 by establishing a positive feedback loop. However, for high-low input transition, initially, N_2 is off and P_2 is on, while for low-high input transition, initially N_2 is on and P_2 is off. Effectively, these two situations result in two different trip points of the ST, which characterizes the ST hysteretic operation, However, aiming at sub 100 mV operation will lead to the disappearance of hysteresis as explained in [83].

2) ST SUBTHRESHOLD OPERATION

As previously mentioned, supply voltage reduction is generally advantageous for supply-voltage-constrained applications like energy harvesting systems. However, it is limited by on-to-off current ratios degradation with decreasing supply. Thus, many works showed that the effective on-to-off ratio can be considerably improved while operating with lower supply voltage using the ST structure, which reduces leakage from the output node effectively and thereby stabilizes the output voltage level [74], [84]. For instance, [85] presented a differential 10-transistor Static Random

Access Memory (SRAM) suitable for subthreshold operation, using ST structure. This SRAM design was implemented in 0.13 μm CMOS technology, showing proper functionality with a 160 mV supply voltage.

Additionally, the authors in [86] presented a minimalist standard cell library based on the classical CMOS ST inverter, optimized for 90 mV supply voltage operation. The robustness of the ST library was verified through the measurement of two frequency divider chains, using either standard or ST logic. The ST logic managed to operate from 76 mV, while the conventional logic operated from 94 mV, which confirms that ST logic allows standard cells operation from very low supply voltages (of the order of 3x the thermal voltage) even though it consumes more area and increases delay as compared to conventional logic. Also, the operation of digital circuits at 62 mV supply voltage was reported in [74] without extra process or post-silicon tuning by using ST. Therefore, ST is an effective solution for mitigating global variations and decreasing supply voltage requirements, while keeping an effective on-to-off ratio, in start-up circuits. This is of great significance in our case, since it can yield an effective RO operating well in the subthreshold region [87].

FIGURE 17. Selective ST delay element from [90].

3) ST ADVANTAGES IN SUBTHRESHOLD REGION

First, ST voltage gain is much higher than that of the conventional inverter. However, this comes at the expense of a larger area occupied by the ST and lower operating frequency at the same supply voltage. Nevertheless, at considerably high supply voltage, the size of the transistors tends to be lower, which means that the occupied area and operating frequency of the ST tend to be similar to that of the conventional inverter. Additionally, the ST is less sensitive to process, voltage, and temperature (PVT) variations, and it can work as an inverter at very low supply voltages, even in the presence of PVT variations, because its Voltage Transfer Curve (VTC) is well defined. Moreover, the optimized ST can theoretically operate at 31.5 mV supply voltage at 300 K (provide a voltage gain higher than unity), which is slightly lower than the conventional inverter (36 mV). This result is significant because it sets a new limit for the lower bound of the supply voltage needed for ultralow-voltage circuits. However, careful analysis of surrounding circuits is required since the static noise margin of the ST is higher than the conventional inverter, and noise present in the circuits tends to disturb their operation [30], [88], [89]. Thus, there have been some attempts to build ROs from STs to operate in the subthreshold region.

4) ST-BASED RO

A comparison in [83] was reported between the ST and the inverter-based ROs. Results showed that for V_{DD} = 70 mV, the inverter-based RO had 43.36 mV output voltage swing, and the ST-based RO had 54.34 mV output voltage swing.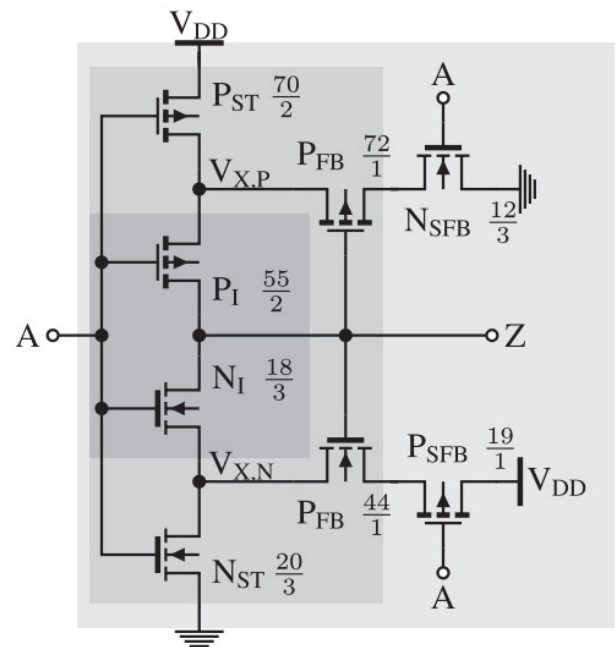 Furthermore, inverter-based ROs did not oscillate at supply voltages below 70 mV due to low voltage gain. However, the ST-based RO oscillated at a supply voltage of 57 mV.

5) SELF-BIASED ST-BASED RO

Moreover, authors in [88] demonstrated through simulations that self-biased ST-based RO (which uses STs as basic cells, along with self-biasing by connecting the substrates to the gates) can reach start-up voltages of around 40 mV. Additionally, they demonstrated experimentally that it can start up from supply voltages of around 50 mV. In particular, it managed to reduce the minimum supply voltage by 5 to 6 mV in comparison with the stacked-inverter RO presented in [76].

6) SELECTIVE ST-BASED RO

Furthermore, a modified ST (Selective ST (SST)-logic) was presented in [90]. The SST cell, as shown in Fig. 17, employs a standard ST cell, but adds two extra switches in each feedback branch, and is derived by input signal A. This strengthens the leakage suppression explained for standard ST cells. The SST logic was utilized in startup control circuitry (9-stage RO) and ultra-low voltage charge pump driving circuits optimized for driving capacitive loads. Consequently, the inductive DC-DC boost converter could reach a minimum startup voltage of 70 mV using a TEG.

IV. SUMMARY OF SIGNIFICANT RESULTS FOUND IN THE LITERATURE

Several start-up approaches for DC energy harvesting (EH) technologies (TEGs considered as the primary example) were presented in this paper. Each method offers some advantages and also suffers from some limitations as summarized in

TABLE 2. Overview of the reviewed subthreshold ring oscillators for start-up circuits.

Ref.	Year	Technology	RO delay cell	number Of stages	Area (μm^2)	RO minimum supply voltage (mV)	Application	Results type
[75]	2020	180 nm CMOS	Self-Bias Feedback Inverter	31	15,298	42	RO	Measurements
[76]	2019	180 nm CMOS	Stacked Three-Inverter Cell	21	14,991	40	TEG start-up	Measurements
[77]	2023	180 nm BCD CMOS	Variants of Body-Biased Stacked Three-Inverter Cell	13	5,875	32.5	RO	Post-layout simulations
[78]	2023	180 nm,1 poly, 6 metal CMOS with deep N-well option	Recursive Body-Biased Stacked Three-Inverter Cell	41	123,000	30	RO	Measurements
[79]	2018	65 nm CMOS	Redundant Inverter Cell	11	915,920*	45	TEG start-up	Measurements
[80]	2020	180 nm CMOS with deep N-well option	Stacked Three-Inverter Cell + Self-Bias Feedback Inverter	27	25,600	34	RO	Pre-layout simulations
[91]	2021	180 nm CMOS with deep N-well option	Stacked Three-Inverter Cell + Self-Bias Feedback Inverter	27	26,000	35	RO	Measurements
[58]	2020	180 nm CMOS	Stacked Three-Inverter Cell + Dynamic Body Biasing	21	28,050	36	RO	Post-layout simulations
[81]	2018	180 nm CMOS	Process Tolerant Inverter Cell	11 (with corner detection circuit)	2,760,000*	50	TEG start-up	Measurements
[19]	2016	180 nm CMOS	Feedback Body Biasing Inverter cell	5 (with 8 stage buffer)	61,040**	60	TEG start-up	Post-layout simulations
[88]	2019	130 nm CMOS	ST + Dynamic Body Biasing	13	N/A	53.2	RO	Post-layout simulations
[83]	2017	180 nm CMOS	ST	3	N/A	57	RO	Post-layout simulations
[90]	2016	130 nm CMOS	Selective ST	9	151,856 *	60	TEG start-up	Measurements

* The area of the startup circuit including the ring oscillator.
** The area estimated from dimensions (including the buffers).

Table 1. The "External Battery" approach is the simplest start-up solution. However, unreliability and high cost render it unsuitable for EH applications. On the other hand, the "Extra-Fabrication-Process based" approach is more suitable for EH applications as it enables low start-up voltages without the need for external components. Nevertheless, it is not compatible with standard CMOS technologies. Both "Transformers" and "Multisource Energy Harvesting" approaches allow very Low start-up voltage with high reliability, however, the added complexity and area overhead of bulky external components pose a serious challenge. Moreover, attempts to implement integrated versions still suffer from severe efficiency degradation. Finally, the "DC-AC-DC Conversion Using Oscillators" approach has two effective oscillator categories: the first is using an LC tank Oscillator; which resembles the "Transformers" approach in both merits and limitations. The second is using RO; which is considered the most promising solution as it is fully integrated with good performance, compatible with regular CMOS technology, less expensive, and needs only one

energy source without compromising reliability. However, to implement an effective RO start-up solution for energy-constrained-harvesting applications, a simple inverter as the delay element in a conventional RO will not suffice because it requires a large supply voltage (a few hundred millivolts) to ensure the correct logic operation. Consequently, many researchers proposed new delay cells, applied new biasing mechanisms, or combined both. The most significant results from the past 10 years were analyzed and then summarised in Table 2. Process Tolerant Inverter presented in [81] provides a reliable solution to start up from low voltage. However, it is possible to harness the same effect by designing the RO using Fully Depleted Silicon On Insulator (FDSOI) technology, which plays a robust role in minimizing process variations without complexity, area, and power overhead of a corner detection circuit; since the power constraint is strict in energy harvesting systems. Employing a Feedback inverter for body biasing is considered effective in lowering transistors threshold value and lowering the minimum supply voltage subsequently. Nevertheless, this doubles the number of stages in the RO and increases power consumption. Thus, we believe dynamic body biasing is more suitable as implemented in [58]. Moreover, dynamic body biasing combined with either the "Stacked Three-Inverter" cell [58] or "ST" cell yields promising results as both cells provide high performance in the subthreshold region due to advanced leakage suppression. The area overhead can be neglected as the final solution will be fully integrated but present similar results to approaches that employ Off-chip components.

In general, for DC EH applications where reliability and low supply voltage is of greater significance regardless of the area, the "Transformers" approach is believed to be the best suited, while for DC EH applications where small size is critical, the most suitable technique is RO start-up using stacked three-inverter or ST cell combined with dynamic body biasing regardless of the used technology, however, the FD-SOI technology is advisable as it minimizes process variations and allows more effective dynamic body biasing.

V. CONCLUSION

Several start-up solutions for DC energy harvesting technologies (with TEGs considered as primary examples) have been reviewed in this paper. Different solutions have been categorized into 5 main approaches as those using: External Battery, Extra-Fabrication-Process based, Transformers, Multisource Energy Harvesting, and DC-AC-DC Conversion Using Oscillators. The "DC-AC-DC Conversion ROs" approach is considered the most promising in line with DC energy harvesting applications because it has several advantages over other approaches such as being fully integrated with good performance, compatible with regular CMOS technology, less expensive, and it needs only one energy source without compromising reliability. Finally, we evaluated various "DC-AC-DC Conversion ROs" implementations to identify their respective advantages and limitations. The overall perspective provided by this review

can be used as a foundation to propose better energy harvesting solutions.

REFERENCES

[1] M. Haras and T. Skotnicki, "Thermoelectricity for IoT—A review," *Nano Energy*, vol. 54, pp. 461–476, Dec. 2018.

[2] Q. F. Hassan, S. A. Madani, and A. U. R. Khan, *Internet of Things: Challenges, Advances, and Applications*. Evanston, IL, USA: Routledge, 2017.

[3] C. Perera, *Sensing As a Service for Internet of Things: A Roadmap*. Victoria, BC, Canada: Leanpub, 2018.

[4] A. Kumar, A. Singh, A. Kumar, M. K. Singh, P. Mahanta, and S. C. Mukhopadhyay, "Sensing technologies for monitoring intelligent buildings: A review," *IEEE Sensors J.*, vol. 18, no. 12, pp. 4847–4860, Jun. 2018.

[5] D. Newell and M. Duffy, "Review of power conversion and energy management for low-power, low-voltage energy harvesting powered wireless sensors," *IEEE Trans. Power Electron.*, vol. 34, no. 10, pp. 9794–9805, Oct. 2019.

[6] K.-S. Ha et al., "23.1 A 7.5 Gb/s/pin LPDDR5 SDRAM with WCK clocking and non-target ODT for high speed and with DVFS, internal data copy, and deep-sleep mode for low power," in *IEEE Int. Solid-State Circuits Conf. (ISSCC) Dig. Tech. Papers*, Feb. 2019, pp. 378–380.

[7] S. Pan and P. K. T. Mok, "A 10-MHz hysteretic-controlled buck converter with single on/off reference tracking using turning-point prediction for DVFS application," *IEEE Trans. Circuits Syst. I, Reg. Papers*, vol. 66, no. 11, pp. 4502–4515, Nov. 2019.

[8] H.-H. Lee, C.-W. Liu, M. Takamiya, and P.-H. Chen, "Single-inductor dual-input dual-output battery-PV hybrid system with 2-D adaptive on-time control for Internet of Things," *IEEE Trans. Circuits Syst. I, Reg. Papers*, vol. 67, no. 3, pp. 1069–1078, Mar. 2020.

[9] O. O. Akintade, T. K. Yesufu, and L. O. Kehinde, "Development of power consumption models for ESP8266-enabled low-cost IoT monitoring nodes," *Adv. Internet Things*, vol. 09, no. 1, pp. 1–14, 2019.

[10] C. Fluur, K. Bolse, A. Strömberg, and I. Thylén, "Patients' experiences of the implantable cardioverter defibrillator (ICD); With a focus on battery replacement and end-of-life issues," *Heart Lung*, vol. 42, no. 3, pp. 202–207, May 2013.

[11] A. Patil, V. Patil, D. Wook Shin, J.-W. Choi, D.-S. Paik, and S.-J. Yoon, "Issue and challenges facing rechargeable thin film lithium batteries," *Mater. Res. Bull.*, vol. 43, nos. 8–9, pp. 1913–1942, Aug. 2008.

[12] S. Priya and D. J. Inman, *Energy Harvesting Technologies*, vol. 21. New York, NY, USA: Springer, 2009.

[13] S. Sudevalayam and P. Kulkarni, "Energy harvesting sensor nodes: Survey and implications," *IEEE Commun. Surveys Tuts.*, vol. 13, no. 3, pp. 443–461, 3rd Quart., 2011.

[14] H. Reinisch, S. Gruber, H. Unterassinger, M. Wiessflecker, G. Hofer, W. Pribyl, and G. Holweg, "An electro-magnetic energy harvesting system with 190 nW idle mode power consumption for a BAW based wireless sensor node," *IEEE J. Solid-State Circuits*, vol. 46, no. 7, pp. 1728–1741, Jul. 2011.

[15] I. Demirkol, D. Camps-Mur, J. Paradells, M. Combalia, W. Popoola, and H. Haas, "Powering the Internet of Things through light communication," *IEEE Commun. Mag.*, vol. 57, no. 6, pp. 107–113, Jun. 2019.

[16] S. Mondal and R. Paily, "On-chip photovoltaic power harvesting system with low-overhead adaptive MPPT for IoT nodes," *IEEE Internet Things J.*, vol. 4, no. 5, pp. 1624–1633, Oct. 2017.

[17] G. Saini, L. Somappa, and M. S. Baghini, "A 500-nW-to-1-mW input power inductive boost converter with MPPT for RF energy harvesting system," *IEEE J. Emerg. Sel. Topics Power Electron.*, vol. 9, no. 5, pp. 5261–5271, Oct. 2021.

[18] K. K. Pakkirisami Churchill, G. Chong, H. Ramiah, M. Y. Ahmad, and J. Rajendran, "Low-voltage capacitive-based step-up DC–DC converters for RF energy harvesting system: A review," *IEEE Access*, vol. 8, pp. 186393–186407, 2020.

[19] M. Ashraf and N. Masoumi, "A thermal energy harvesting power supply with an internal startup circuit for pacemakers," *IEEE Trans. Very Large Scale Integr. (VLSI) Syst.*, vol. 24, no. 1, pp. 26–37, Jan. 2016.

[20] J. Iannacci, "Microsystem based energy harvesting (EH-MEMS): Powering pervasivity of the Internet of Things (IoT)—A review with focus on mechanical vibrations," *J. King Saud Univ. Sci.*, vol. 31, no. 1, pp. 66–74, Jan. 2019.

[21] D. Bouchouicha, F. Dupont, M. Latrach, and L. Ventura, "Ambient RF energy harvesting," in *Proc. Int. Conf. Renew. Energies Power Qual.*, vol. 13, 2010, pp. 2–6.

[22] A. Cuadras, M. Gasulla, and V. Ferrari, "Thermal energy harvesting through pyroelectricity," *Sens. Actuators A, Phys.*, vol. 158, no. 1, pp. 132–139, Mar. 2010.

[23] X. Lu and S.-H. Yang, "Thermal energy harvesting for WSNs," in *Proc. IEEE Int. Conf. Syst., Man Cybern.*, Oct. 2010, pp. 3045–3052.

[24] R. Dekimpe, P. Xu, M. Schramme, P. Gérard, D. Flandre, and D. Bol, "A battery-less BLE smart sensor for room occupancy tracking supplied by 2.45-GHz wireless power transfer," *Integration*, vol. 67, pp. 8–18, Jul. 2019.

[25] R. Dekimpe, P. Xu, M. Schramme, D. Flandre, and D. Bol, "A battery-less BLE IoT motion detector supplied by 2.45-GHz wireless power transfer," in *Proc. 28th Int. Symp. Power Timing Model., Optim. Simul. (PATMOS)*, Jul. 2018, pp. 68–75.

[26] S. Shen, Y. Zhang, C.-Y. Chiu, and R. Murch, "Directional multiport ambient RF energy-harvesting system for the Internet of Things," *IEEE Internet Things J.*, vol. 8, no. 7, pp. 5850–5865, Apr. 2021.

[27] S. Mandal and R. Sarpeshkar, "Low-power CMOS rectifier design for RFID applications," *IEEE Trans. Circuits Syst. I, Reg. Papers*, vol. 54, no. 6, pp. 1177–1188, Jun. 2007.

[28] T. Le, K. Mayaram, and T. Fiez, "Efficient far-field radio frequency energy harvesting for passively powered sensor networks," *IEEE J. Solid-State Circuits*, vol. 43, no. 5, pp. 1287–1302, May 2008.

[29] K. Kotani, A. Sasaki, and T. Ito, "High-efficiency differential-drive CMOS rectifier for UHF RFIDs," *IEEE J. Solid-State Circuits*, vol. 44, no. 11, pp. 3011–3018, Nov. 2009.

[30] J. V. T. Ferreira and C. Galup-Montoro, "Ultra-low-voltage CMOS ring oscillators," *Electron. Lett.*, vol. 55, no. 9, pp. 523–525, May 2019.

[31] C. R. Bowen, J. Taylor, E. LeBoulbar, D. Zabek, A. Chauhan, and R. Vaish, "Pyroelectric materials and devices for energy harvesting applications," *Energy Environ. Sci.*, vol. 7, no. 12, pp. 3836–3856, 2014.

[32] H. Jouhara, A. Żabnieńska-Góra, N. Khordehgah, Q. Doraghi, L. Ahmad, L. Norman, B. Axcell, L. Wrobel, and S. Dai, "Thermoelectric generator (TEG) technologies and applications," *Int. J. Thermofluids*, vol. 9, Feb. 2021, Art. no. 100063.

[33] M. Jaworski, M. Bednarczyk, and M. Czachor, "Experimental investigation of thermoelectric generator (TEG) with PCM module," *Appl. Thermal Eng.*, vol. 96, pp. 527–533, Mar. 2016.

[34] M.-K. Kim, M.-S. Kim, S. Lee, C. Kim, and Y.-J. Kim, "Wearable thermoelectric generator for harvesting human body heat energy," *Smart Mater. Struct.*, vol. 23, no. 10, Oct. 2014, Art. no. 105002.

[35] C. Lu, V. Raghunathan, and K. Roy, "Efficient design of micro-scale energy harvesting systems," *IEEE J. Emerg. Sel. Topics Circuits Syst.*, vol. 1, no. 3, pp. 254–266, Sep. 2011.

[36] V. Priya, M. K. Rajendran, S. Kansal, G. Chowdary, and A. Dutta, "A human body heat driven high throughput thermal energy harvesting single stage regulator for wearable biomedical IoT nodes," *IEEE Internet Things J.*, vol. 5, no. 6, pp. 4989–5001, Dec. 2018.

[37] B. Wang, Y. Hong, Z. Long, Q. Pan, P. Li, Y. Xi, and Z. Yang, "Characterization of wrist motions and bionic energy harvesting for wrist wearables," *IEEE Internet Things J.*, vol. 9, no. 21, pp. 21147–21156, Nov. 2022.

[38] T. Hendricks and W. T. Choate. (Nov. 2006). *Engineering Scoping Study of Thermoelectric Generator Systems for Industrial Waste Heat Recovery.* [Online]. Available: https://www.osti.gov/biblio/1218711

[39] J. Yan, X. Liao, D. Yan, and Y. Chen, "Review of micro thermoelectric generator," *J. Microelectromech. Syst.*, vol. 27, no. 1, pp. 1–18, Feb. 2018.

[40] S. Lan, Z. Yang, R. Chen, and R. Stobart, "A dynamic model for thermoelectric generator applied to vehicle waste heat recovery," *Appl. Energy*, vol. 210, pp. 327–338, Jan. 2018.

[41] K. Nemoto, R. Takeuchi, M. Baba, M. Takeda, and N. Yamada, "Output power leveling of on-chip thermoelectric generator using a solid–solid phase change material," *J. Energy Storage*, vol. 56, Dec. 2022, Art. no. 106119.

[42] M. Strasser, R. Aigner, C. Lauterbach, T. F. Sturm, M. Franosch, and G. Wachutka, "Micromachined CMOS thermoelectric generators as on-chip power supply," *Sens. Actuators A, Phys.*, vol. 114, nos. 2–3, pp. 362–370, Sep. 2004.

[43] K. Y. Lee, D. Brown, and S. Kumar, "Silicon nanowire arrays based on-chip thermoelectric generators," *IEEE Trans. Compon., Packag., Manuf. Technol.*, vol. 5, no. 8, pp. 1100–1107, Aug. 2015.

[44] A. Nozariasbmarz, H. Collins, K. Dsouza, M. H. Polash, M. Hosseini, M. Hyland, J. Liu, A. Malhotra, F. M. Ortiz, F. Mohaddes, V. P. Ramesh, Y. Sargolzaeiaval, N. Snouwaert, M. C. Öztürk, and D. Vashaee, "Review of wearable thermoelectric energy harvesting: From body temperature to electronic systems," *Appl. Energy*, vol. 258, Jan. 2020, Art. no. 114069.

[45] M. M. Camboim, V. S. Oliveira, M. R. Villarim, A. W. R. Villarim, S. Y. C. Catunda, O. R. Baiocchi, and C. P. de Souza, "An online remote verification system of thermal sources for energy harvesting application," *IEEE Trans. Instrum. Meas.*, vol. 69, no. 10, pp. 7962–7973, Oct. 2020.

[46] M. Alhawari, B. Mohammad, H. Saleh, and M. Ismail, "An efficient polarity detection technique for thermoelectric harvester in L-based converters," *IEEE Trans. Circuits Syst. I, Reg. Papers*, vol. 64, no. 3, pp. 705–716, Mar. 2017.

[47] Y. K. Ramadass and A. P. Chandrakasan, "A battery-less thermoelectric energy harvesting interface circuit with 35 mV startup voltage," *IEEE J. Solid-State Circuits*, vol. 46, no. 1, pp. 333–341, Jan. 2011.

[48] S. Lineykin and S. Ben-Yaakov, "Modeling and analysis of thermoelectric modules," *IEEE Trans. Ind. Appl.*, vol. 43, no. 2, pp. 505–512, 2007.

[49] R. P. Rocha, J. P. Carmo, L. M. Goncalves, and J. H. Correia, "An energy scavenging microsystem based on thermoelectricity for battery life extension in laptops," in *Proc. 35th Annu. Conf. IEEE Ind. Electron.*, Nov. 2009, pp. 1813–1816.

[50] L. Chen, D. Cao, Y. Huang, and F. Z. Peng, "Modeling and power conditioning for thermoelectric generation," in *Proc. IEEE Power Electron. Specialists Conf.*, Jun. 2008, pp. 1098–1103.

[51] Y. Yang, X.-J. Wei, and J. Liu, "Suitability of a thermoelectric power generator for implantable medical electronic devices," *J. Phys. D, Appl. Phys.*, vol. 40, no. 18, pp. 5790–5800, Sep. 2007.

[52] O. H. Ando Junior, A. L. O. Maran, and N. C. Henao, "A review of the development and applications of thermoelectric microgenerators for energy harvesting," *Renew. Sustain. Energy Rev.*, vol. 91, pp. 376–393, Aug. 2018.

[53] J.-P. Im, S.-W. Wang, S.-T. Ryu, and G.-H. Cho, "A 40 mV transformer-reuse self-startup boost converter with MPPT control for thermoelectric energy harvesting," *IEEE J. Solid-State Circuits*, vol. 47, no. 12, pp. 3055–3067, Dec. 2012.

[54] P.-H. Chen, K. Ishida, K. Ikeuchi, X. Zhang, K. Honda, Y. Okuma, Y. Ryu, M. Takamiya, and T. Sakurai, "Startup techniques for 95 mV step-up converter by capacitor pass-on scheme and V_{TH}-tuned oscillator with fixed charge programming," *IEEE J. Solid-State Circuits*, vol. 47, no. 5, pp. 1252–1260, May 2012.

[55] P.-H. Chen, T.-Y. Su, and P. M. Fan, "Thermoelectric energy harvesting interface circuit with capacitive bootstrapping technique for energy-efficient IoT devices," *IEEE Internet Things J.*, vol. 5, no. 5, pp. 4058–4065, Oct. 2018.

[56] E. J. Carlson, K. Strunz, and B. P. Otis, "A 20 mV input boost converter with efficient digital control for thermoelectric energy harvesting," *IEEE J. Solid-State Circuits*, vol. 45, no. 4, pp. 741–750, Apr. 2010.

[57] I. Doms, P. Merken, C. Van Hoof, and R. P. Mertens, "Capacitive power management circuit for micropower thermoelectric generators with a 1.4 μA controller," *IEEE J. Solid-State Circuits*, vol. 44, no. 10, pp. 2824–2833, Oct. 2009.

[58] Z. Xie, Z. Wu, and J. Wu, "Low voltage delay element with dynamic biasing technique for fully integrated cold-start in battery-assistance DC energy harvesting systems," *Appl. Sci.*, vol. 10, no. 19, p. 6993, Oct. 2020.

[59] Y.-K. Teh and P. K. T. Mok, "DTMOS-based pulse transformer boost converter with complementary charge pump for multisource energy harvesting," *IEEE Trans. Circuits Syst. II, Exp. Briefs*, vol. 63, no. 5, pp. 508–512, May 2016.

[60] Y.-K. Teh and P. K. T. Mok, "Design of transformer-based boost converter for high internal resistance energy harvesting sources with 21 mV self-startup voltage and 74% power efficiency," *IEEE J. Solid-State Circuits*, vol. 49, no. 11, pp. 2694–2704, Nov. 2014.

[61] *Ultralow Voltage Step-Up Converter and Power Manager Features*, document LTC3108, Linear Technol. Corp., Milpitas, CA, USA, 2013.

[62] H. Zhang, M. Zhao, S. Liu, and X. Wu, "A new transformer-based startup scheme with novel voltage monitors for energy harvesting," in *Proc. IEEE Int. Conf. Electron Devices Solid-State Circuits*, Jun. 2014, pp. 1–2.

[63] Y. Qian, D. Lu, J. He, and Z. Hong, "An on-chip transformer-based self-startup hybrid SIDITO converter for thermoelectric energy harvesting," *IEEE Trans. Circuits Syst. II, Exp. Briefs*, vol. 65, no. 11, pp. 1673–1677, Nov. 2018.

[64] H. Fuketa, S.-I. O'uchi, and T. Matsukawa, "Fully integrated, 100-mV minimum input voltage converter with gate-boosted charge pump kick-started by LC oscillator for energy harvesting," *IEEE Trans. Circuits Syst. II, Exp. Briefs*, vol. 64, no. 4, pp. 392–396, Apr. 2017.

[65] H. Fuketa, Y. Momiyama, A. Okamoto, T. Sakata, M. Takamiya, and T. Sakurai, "An 85-mV input, 50-μs startup fully integrated voltage multiplier with passive clock boost using on-chip transformers for energy harvesting," in *Proc. 40th Eur. Solid State Circuits Conf. (ESSCIRC)*, Sep. 2014, pp. 263–266.

[66] Y. Zhang, F. Zhang, Y. Shakhsheer, J. D. Silver, A. Klinefelter, M. Nagaraju, J. Boley, J. Pandey, A. Shrivastava, E. J. Carlson, A. Wood, B. H. Calhoun, and B. P. Otis, "A batteryless 19 μW MICS/ISM-band energy harvesting body sensor node SoC for ExG applications," *IEEE J. Solid-State Circuits*, vol. 48, no. 1, pp. 199–213, Jan. 2013.

[67] Z. Liu, Y.-P. Hsu, and M. M. Hella, "A thermal/RF hybrid energy harvesting system with rectifying-combination and improved fractional-OCV MPPT method," *IEEE Trans. Circuits Syst. I, Reg. Papers*, vol. 67, no. 10, pp. 3352–3363, Oct. 2020.

[68] L. Guo, X. Gu, P. Chu, S. Hemour, and K. Wu, "Collaboratively harvesting ambient radiofrequency and thermal energy," *IEEE Trans. Ind. Electron.*, vol. 67, no. 5, pp. 3736–3746, May 2020.

[69] P.-S. Weng, H.-Y. Tang, P.-C. Ku, and L.-H. Lu, "50 mV-input batteryless boost converter for thermal energy harvesting," *IEEE J. Solid-State Circuits*, vol. 48, no. 4, pp. 1031–1041, Apr. 2013.

[70] V. Thakur and V. Verma, "Low power consumption differential ring oscillator," *Int. J. Electron. Commun. Eng.*, vol. 6, no. 1, pp. 81–92, 2013.

[71] R. L. Radin, M. Sawan, C. Galup-Montoro, and M. C. Schneider, "A 7.5-mV-input boost converter for thermal energy harvesting with 11-mV self-startup," *IEEE Trans. Circuits Syst. II, Exp. Briefs*, vol. 67, no. 8, pp. 1379–1383, Aug. 2020.

[72] M. Bender Machado and R. Luciano Radin, "Overview of sub-100 mV oscillators," *J. Integr. Circuits Syst.*, vol. 17, no. 1, pp. 1–8, Apr. 2022.

[73] T. Tran-Dinh, H. M. Pham, L. Pham-Nguyen, S.-G. Lee, and H.-P. Le, "Power management IC with a three-phase cold self-start for thermoelectric generators," *IEEE Trans. Circuits Syst. I, Reg. Papers*, vol. 68, no. 1, pp. 103–113, Jan. 2021.

[74] N. Lotze and Y. Manoli, "A 62 mV 0.13 μm CMOS standard-cell-based design technique using Schmitt-trigger logic," *IEEE J. Solid-State Circuits*, vol. 47, no. 1, pp. 47–60, Jan. 2012.

[75] R. Matsuzuka, T. Terada, K. Matsumoto, M. Kitamura, and T. Hirose, "A 42 mV startup ring oscillator using gain-enhanced self-bias inverters for extremely low voltage energy harvesting," *Jpn. J. Appl. Phys.*, vol. 59, no. SG, Apr. 2020, Art. no. SGGL01.

[76] S. Bose, T. Anand, and M. L. Johnston, "Integrated cold start of a boost converter at 57 mV using cross-coupled complementary charge pumps and ultra-low-voltage ring oscillator," *IEEE J. Solid-State Circuits*, vol. 54, no. 10, pp. 2867–2878, Oct. 2019.

[77] A. Mukherjee, A. C. Jayamon, R. S. C. Teja, and A. Dutta, "Ultra-low voltage start-up clock generators for micro-scale energy harvesting: New variants of body-biased stacked inverter based ring oscillators," *Microelectron. J.*, vol. 139, Sep. 2023, Art. no. 105883.

[78] H. Sebe, T. Okumura, S. Sumi, D. Kanemoto, P.-H. Chen, and T. Hirose, "Sub-30-mV-supply, fully integrated ring oscillator consisting of recursive stacking body-bias inverters for extremely low-voltage energy harvesting," in *Proc. IEEE 49th Eur. Solid State Circuits Conf. (ESSCIRC)*, Sep. 2023, pp. 325–328.

[79] Z. Luo, L. Zeng, B. Lau, Y. Lian, and C.-H. Heng, "A sub-10 mV power converter with fully integrated self-start, MPPT, and ZCS control for thermoelectric energy harvesting," *IEEE Trans. Circuits Syst. I, Reg. Papers*, vol. 65, no. 5, pp. 1744–1757, May 2018.

[80] M. Nishi, K. Matsumoto, N. Kuroki, M. Numa, H. Sebe, R. Matsuzuka, O. Maida, D. Kanemoto, and T. Hirose, "A 34-mV startup ring oscillator using stacked body bias inverters for extremely low-voltage thermoelectric energy harvesting," in *Proc. 18th IEEE Int. New Circuits Syst. Conf. (NEWCAS)*, Jun. 2020, pp. 38–41.

[81] M. Dezyani, H. Ghafoorifard, S. Sheikhaei, and W. A. Serdijn, "A 60 mV input voltage, process tolerant start-up system for thermoelectric energy harvesting," *IEEE Trans. Circuits Syst. I, Reg. Papers*, vol. 65, no. 10, pp. 3568–3577, Oct. 2018.

[82] T. Fernandes, M. C. Schneider, and D. V. Lettnin, "CMOS amplifiers and Schmitt triggers for ultra-low-voltage applications," M.S. thesis, Universidade Federal de Santa Catarina (UFSC), Florianópolis, Brazil, 2019.

[83] L. A. P. Melek, A. L. da Silva, M. C. Schneider, and C. Galup-Montoro, "Analysis and design of the classical CMOS Schmitt trigger in subthreshold operation," *IEEE Trans. Circuits Syst. I, Reg. Papers*, vol. 64, no. 4, pp. 869–878, Apr. 2017.

[84] R. L. Radin, M. B. Machado, M. Sawan, C. Galup-Montoro, and M. C. Schneider, "Ultra-low-voltage oscillators," in *Ultra-Low Voltage Circuit Techniques for Energy Harvesting*. Cham, Switzerland: Springer, 2022, pp. 25–52.

[85] J. P. Kulkarni, K. Kim, and K. Roy, "A 160 mV robust Schmitt trigger based subthreshold SRAM," *IEEE J. Solid-State Circuits*, vol. 42, no. 10, pp. 2303–2313, Oct. 2007.

[86] D. G. A. Neto and C. Galup-Montoro, "Design and testing of a 32-kHz frequency divider chain operating at VDD = 76 mV," in *Proc. IEEE Int. Symp. Circuits Syst. (ISCAS)*, Oct. 2020, pp. 1–5.

[87] A. Nowbahari, L. Marchetti, and M. Azadmehr, "Weak inversion model of an inverting CMOS Schmitt trigger," in *Proc. 11th Int. Conf. Commun., Circuits Syst. (ICCCAS)*, May 2022, pp. 1–5.

[88] L. A. Pasini Melek, M. C. Schneider, and C. Galup-Montoro, "Operation of the classical CMOS Schmitt trigger as an ultra-low-voltage amplifier," *IEEE Trans. Circuits Syst. II, Exp. Briefs*, vol. 65, no. 9, pp. 1239–1243, Sep. 2018.

[89] L. A. P. Melek, "Analysis and design of a subthreshold CMOS Schmitt trigger circuit," Ph.D. thesis, Universidade Federal de Santa Catarina, Florianópolis, Brazil, 2017.

[90] J. Goeppert and Y. Manoli, "Fully integrated startup at 70 mV of boost converters for thermoelectric energy harvesting," *IEEE J. Solid-State Circuits*, vol. 51, no. 7, pp. 1716–1726, Jul. 2016.

[91] M. Nishi, K. Matsumoto, N. Kuroki, M. Numa, H. Sebe, R. Matsuzuka, O. Maida, D. Kanemoto, and T. Hirose, "A 35-mV supply ring oscillator consisting of stacked body bias inverters for extremely low-voltage LSIs," *IEICE Electron. Exp.*, vol. 18, no. 6, 2021, Art. no. 20210065.

MAHMOUD AHMED (Member, IEEE) received the B.S. degree in electrical engineering from the Zewail City of Science and Technology, Giza, Egypt, in 2020. He is currently pursuing the Ph.D. degree with the Department of Electrical Engineering, Polytechnique Montréal, Canada. In 2021, he was an Electrical Engineering Intern with Dolphin Design, Meylan, France, and worked on TEG power conditioning design. His current research interests include analog, RF, and mixed-signal design.

SEBASTIEN GENEVEY received the degree in electronics and microelectronics engineering from the Polytechnic Institute of Montpellier, France. Since 1997, he has been with Dolphin Design (formerly Dolphin Integration) as an Analog and Mixed-Signal Architect for different product lines, from audio to power management.

MOHAMED ALI (Member, IEEE) received the B.Sc. degree in electronics from the Faculty of Electronics Engineering, Menoufia University, Egypt, in 2005, the M.Sc. degree in electronics and communication engineering from Ain Shams University, Egypt, in 2011, and the joint Ph.D. degree in electronics and communication engineering from Ain Shams University, jointly with Polytechnique Montréal, Québec City, Canada, in 2017. From 2015 to 2017, he was a Research Intern with Polytechnique Montréal, as a part of his Ph.D. Program. Since 2007, he has been with the Microelectronics Department, Electronics Research Institute, Cairo, Egypt. Since 2018, he has been a Post-Doctoral Fellow with the Department of Electrical Engineering, Polytechnique Montréal. He is currently a Staff Analog and Mixed-Signal Design Engineer with Synopsys Inc., Ottawa, Canada. His research interests include analog, RF, mixed-signal design, systems-on-chip, power management implementations, and analog circuits for high-speed wireline transceivers.

YVON SAVARIA (Life Fellow, IEEE) received the B.Ing. and M.Sc.A. degrees in electrical engineering from Polytechnique Montréal, Montreal, QC, Canada, in 1980 and 1982, respectively, and the Ph.D. degree in electrical engineering from McGill University, Montreal, in 1985. He has been a Consultant or was sponsored for carrying out research with Bombardier, Buspass, CNRC, Design Workshop, Dolphin, DREO, Ericsson, Genesis, Gennum, Huawei, Hyperchip, Intel, ISR, Kaloom, LTRIM, Miranda, MiroTech, Nortel, Octasic, PMC-Sierra, Space Codesign, Technocap, Thales, Tundra, and Wavelite. Since 1985, he has been with Polytechnique Montréal, where he is currently a Professor with the Department of Electrical Engineering. He is involved in several projects related to embedded systems in aircraft, wireless sensor networks, virtual networks, software-defined networks, machine learning (ML), embedded ML, computational efficiency, and application-specific architecture design. He holds 16 patents, has published 190 journal articles and 485 conference papers, and was the Thesis Advisor of 190 graduate students who completed their studies. He has carried out work in several areas related to microelectronic circuits and microsystems such as testing, verification, validation, clocking methods, defect and fault tolerance, effects of radiation on electronics, high-speed interconnects, and circuit design techniques, CAD methods, reconfigurable computing and applications of microelectronics to telecommunications, aerospace, image processing, video processing, radar signal processing, and the acceleration of digital signal processing. He is a fellow of Canadian Academy of Engineering and a member of the Executive Committee of the Regroupement Stratégique en Microélectronique du Québec (RESMIQ) and a member of the Ordre des Ingénieurs du Québec (OIQ). In 2001, he was awarded a Tier 1 Canada Research Chair (www.chairs.gc.ca) on the design and architecture of advanced microelectronic systems, in June 2015. He also received a Synergy Award from the Natural Sciences and Engineering Research Council of Canada, in 2006. Since June 2019, he has been the NSERC-Kaloom-Intel-Noviflow (KIN) Chair Professor. He was the Program Co-Chairperson of NEWCAS'2018 and the General Chairperson of NEWCAS'2020.

YVES AUDET (Member, IEEE) received the B.Sc. degree in physics from the University of Sherbrooke, Sherbrooke, QC, Canada, in 1989, the DEA Diploma degree from Joseph Fourier University, Grenoble, France, in 1990, the M.Sc. degree in physics from the University of Sherbrooke in 1992, and the Ph.D. degree from Simon Fraser University, Burnaby, BC, Canada, in 1996, with a focus on large integrated sensor arrays. He was with the Research and Development Group, Mitel Semiconductor, Kanata, ON, Canada, from 1996 to 1999, where he has been involved in the design and characterization of mixed-signal CMOS circuits. Since 2001, he has been a Professor with the Department of Electrical Engineering, Polytechnique Montréal, Montreal, QC, Canada. He has been conducting research projects with many companies, such as Bombardier, MDA, and Thales. His research interests include CMOS sensors, imaging sensors, fault-tolerant circuit architectures, isolation circuits, energy harvesting, and photovoltaic solar systems.

● ● ●